A performance evaluation plot of enhanced heat transfer techniques oriented for energy-saving

J.F. Fan, W.K. Ding, J.F. Zhang, Y.L. He, W.Q. Tao *

School of Energy & Power Engineering, Xi'an Jiaotong University, Xi'an, Shaanxi 710049, PR China

ARTICLE INFO

ABSTRACT

On the basis of the existing performance evaluation criteria analysis and four assumptions, a performance evaluation plot has been proposed in this paper. This plot takes the ratios of heat transfer enhancement and friction factor increase as its two coordinates. The quadrant of the coordinate where both (Nu_e/Nu_0), (f_e/f_0) are greater than 1.0 can be divided into four regions. In Region 1 heat transfer is actually deteriorated based on identical pumping power, in Region 2 heat transfer is enhanced based on identical pumping power but deteriorated based on identical pressure drop, in Region 3 heat transfer is enhanced based on identical pressure drop but the increase in friction factor is larger than the enhancement of heat transfer at identical flow rate, and in Region 4 heat transfer enhancement ratio is larger than friction factor increase ratio based on identical flow rate. For some techniques which lead to the reduction of both heat transfer rate and friction factor, the proposed plot is still applicable. Different enhanced techniques for the same reference one can be easily and clearly compared for their effectiveness when enhancement study is based on energy-saving. Five practical examples are provided to show the functions of the plot.

© 2008 Elsevier Ltd. All rights reserved.

1. Introduction

Heat exchangers are widely used in many engineering fields for the transport of heat (energy) from one fluid to the other. Examples include gas heating in waste heat recovery and gas cooling in intercooler of compressor, refrigerant evaporation and condensation in air-conditioning, liquid heat transfer in chemical and processing equipment, steam generation and condensation in power plants, etc. Heat transfer enhancement techniques provide a powerful tool to improve the thermal performance of heat exchangers, including the reduction of its size and cost, and to save energy for its operation. According to [1], the purposes of heat transfer enhancement study may be classified into four objectives. Simply speaking, they are (1) reducing heat transfer surface area; (2) reducing temperature difference; (3) increasing heat transfer rate; and (4) reducing pumping power. Extensive data have been published on various kinds of heat transfer promoters of heat exchangers [2,3], and all of these heat transfer promoters cause an increase of pressure loss cross the exchanger. It is a common knowledge that the ratio of pressure drop increase is often larger than the ratio of heat transfer enhancement. For example, the very effective offset strip fins used in compact heat exchangers has its ratio of j factor and friction factor j/f being only 80% of that of a plain fin [4], i.e., the increase in the j-factor is only 80% of the increase in pressure drop. Thus with the development of heat transfer enhancement techniques, the question of how to evaluate the enhancement technique is also

brought to attention. A qualitative comparison for enhanced heat transfer surface is an important issue in evaluating the performance improvement of the enhancement techniques. In 1972 Webb and Eckert [5] developed equations to define the performance advantage of roughened tubes in heat exchanger design relative to smooth tubes of equal diameter. To the authors' knowledge this is probably the first paper concerning the evaluation criterion for heat transfer enhancement technique. Since then a great number of evaluation methods have been proposed. These include the 12 combinations for the single-phase flow heat transfer proposed in [1,6]; the criteria based on identical pumping power/identical pressure drop [7–12]; the goodness factor [13,14] used in plate fin–tube surfaces, the criterion based on correlating the heat transfer coefficient and the dissipation energy in a fluid [15]; and the performance assessment methods based on the 2nd law of thermodynamics by computing the entropy generation, or exergy generation in the enhancement processes [16–23]. Broadly speaking, all the existing assessment methods, or criteria, can be classified into two categories. In one category of assessment methods, the 2nd law of the thermodynamics is applied and either entropy or exergy generated is determined, while in the other category discussion is only based on the 1st law of thermodynamics in that no computation of entropy or exergy generation is involved. From an academic point of view the first category seems meaningful, but they have not found wide engineering applications. In this paper, we will concentrate on the second category in the sense that we will not compute exergy or entropy for the comparison purpose, yet we can still identify the effectiveness of an enhancement technique. As indicated in [24], many factors have

---

* Corresponding author.
E-mail address: wqtao@mail.xjtu.edu.cn (W.Q. Tao).

Nomenclature

Latin symbols

A	heat transfer surface area, m^2
Ac	frontal cross-section area, m^2
b	intercept of straight line
c_1, c_2	coefficient in equation
$C_{Q,P}$	the ratio of heat transfer rate between enhanced and reference surfaces under identical pumping power
$C_{Q,V}$	the ratio of heat transfer rate between enhanced and reference surfaces over the ratio of friction factor between enhanced and reference surfaces under identical flow rate
$C_{Q,\Delta p}$	the ratio of heat transfer rate between enhanced and reference surfaces under identical pressure drop
D	hydraulic diameter, m
f	friction factor
h	heat transfer coefficient, $W/(m^2\,K)$
j	j-factor, Colburn factor
k	slope of straight line
L	length of the flow passage, m
Nu	Nusselt number
P	pumping power, W
q	fluid flow rate, kg/s

Q	heat transfer rate, W
Re	Reynolds number
V	flow velocity of fluid, m/s

Greek symbols

Δp	pressure drop, Pa
Δt	wall-to-fluid temperature difference, K
λ	thermal conductivity of fluid, $W/(m\,K)$
ρ	fluid density, kg/m^3

Superscripts

m_1, m_2	exponent in equation

Subscripts

0	reference surface or smooth surface
e	augmented surface
m	mean value
P	under equal pumping power
Re	under equal Reynolds number
V	under equal flow rate
Δp	under equal pressure drop

to be considered in the construction of the assessment criteria, including economic, manufacturability, reliability, and safety, among others. Thus it seems impossible to establish a generally applicable selection criteria [6].

With the emerging of worldwide crises of energy shortage, the energy-saving purpose of heat transfer enhancement has become more crucial and has attracted more and more attention of the international heat transfer community. In this regard, the evaluation approach based in the comparison between enhanced and original (or reference) heat transfer surfaces (or structure) for identical flow rate, identical pressure drop and identical pumping power [7–12] seems more suitable. These criteria will be adopted in this paper.

In another development, for a visual presentation of the performance of heat transfer enhancement technique different kinds of plots have been suggested. These include the plots of heat transfer ratio vs. Reynolds number, the surface area ratio vs. Reynolds number, and the combined *j*-factor, *f*-factor vs. Reynolds number [24]. Among all the existing plots none can be used to indicate whether the heat transmitted per unit pumping power can be increased, or whether the heat transmitted per unit pressure drop can be increased. The major purpose of the present paper is to propose such a plot for the study on heat transfer enhancement techniques oriented towards energy-saving.

In the following presentation, the equations for constructing of such a plot will first be derived, followed by the introduction of the plot components. Following this the application of such a plot will be illustrated taking several existing enhancement techniques as examples. Finally some conclusions will be drawn.

2. The basic equations for constructing performance evaluation plot

First it is to be noted that by performance evaluation we mean the comparison of heat transfer and pressure drop characteristics of an enhanced structure with a reference structure which possesses the same basic dimensions except the part of enhanced structure. As indicated by Marner et al. [25], an equivalent parallel plate duct or an empty tube has often served as such a reference

geometry. For the convenience of presentation, all the physical quantities related to the reference geometry will be denoted by a subscript 0.

To facilitate the comparison process, the performance evaluation is based on the following assumptions:

(1) The thermophysical properties of fluid are constant [1].
(2) Heat transfer area used for calculating the convective heat transfer coefficient of enhanced surface is the same as that of the reference one [1].
(3) The cross-sectional area used for calculating the average velocity of fluid of enhanced surface is the same as that of the reference one.
(4) The reference dimension used for calculating the dimensionless characteristic number of enhanced surface is the same as that of the reference one.

Most of enhanced heat transfer technologies and data reduction methods meet these assumptions in engineering applications, and in some sense, only based on the above assumptions, the performance comparison is meaningful between an enhanced and the reference one.

From our own comparison experiences a convenient and practical way for performance comparison can be made as follows: through experimental or numerical investigations, the ratios of heat transfer and pressure drop of an enhanced surface over the reference one are obtained, and the correlations of friction factor and heat transfer for the reference surface are available, then performance comparison between the two surfaces are conducted in a simple and explicit manner without further computation. In order to construct the performance evaluation plot which can meet the above requirement, derivations of some basic equations are presented as follows.

Assuming that the relevant correlations of the average friction factors and Nusselt number can be fitted for the reference structure as follows:

$$f_0(Re) = c_1 Re^{m_1} \tag{1}$$
$$Nu_0(Re) = c_2 Re^{m_2} \tag{2}$$

At the same Reynolds number Re, the ratios of Nusselt number and friction factor of an enhanced over the reference surface become

$$\left(\frac{f_e}{f_0}\right)_{Re} = \frac{f_e(Re)}{f_0(Re)} \tag{3}$$

$$\left(\frac{Nu_e}{Nu_0}\right)_{Re} = \frac{Nu_e(Re)}{Nu_0(Re)} \tag{4}$$

where the subscript Re means that the ratio is obtained at the same value of Reynolds number for both the enhanced surface and the reference surface.

At different Reynolds numbers, the ratios of Nusselt number and friction factor of the enhanced heat transfer surface over the reference one is expressed by

$$\frac{f_e}{f_0} = \frac{f_e(Re)}{f_0(Re_0)} \tag{5}$$

$$\frac{Nu_e}{Nu_0} = \frac{Nu_e(Re)}{Nu_0(Re_0)} \tag{6}$$

Substituting Eq. (1) into Eq. (3) for $f_0(Re)$, the friction factor of the enhanced surface of Reynolds number Re becomes

$$f_e(Re) = \left(\frac{f_e}{f_0}\right)_{Re} \cdot c_1 Re^{m_1} \tag{7}$$

In order to obtain an expression of friction factor ratio at different Reynolds numbers, substituting Eq. (1) into Eq. (5) for $f_0(Re_0)$ and Eq. (7) into Eq. (5) for $f_e(Re)$, yields

$$\frac{f_e}{f_0} = \frac{f_e(Re)}{f_0(Re_0)} = \left(\frac{f_e}{f_0}\right)_{Re} \left(\frac{Re}{Re_0}\right)^{m_1} \tag{8}$$

Similarly by substituting Eq. (2) into Eq. (4) for $Nu_0(Re)$, the Nusselt number of the enhanced surface at Reynolds number Re becomes

$$Nu_e(Re) = \left(\frac{Nu_e}{Nu_0}\right)_{Re} \cdot c_2 Re^{m_2} \tag{9}$$

Then substituting Eq. (2) into Eq. (6) for $Nu_0(Re_0)$ and Eq. (9) into Eq. (6) for $Nu_e(Re)$, the ratio of the Nusselt number at different Reynolds number can be obtained as follows:

$$\frac{Nu_e}{Nu_0} = \frac{Nu_e(Re)}{Nu_0(Re_0)} = \left(\frac{Nu_e}{Nu_0}\right)_{Re} \left(\frac{Re}{Re_0}\right)^{m_2} \tag{10}$$

Eqs. (8) and (10) are the basic formulations adopted in the construction of the performance evaluation plot. These two equations imply that once the basic correlations of the reference structure and the ratios of friction factors (and Nusselt numbers) of enhanced and reference structures at the same Reynolds number are available, then the two ratios at different Reynolds number can be calculated.

In the performance evaluation of enhanced structure, the ratio of heat transfer rate is of great importance. The expressions of this ratio for the three constraints are derived as follows. According to the definition of pressure drop and pump power consumption [7,24], the ratio of power consumption of enhanced and reference surfaces can be presented as follows:

$$\frac{P_e}{P_0} = \frac{(A_c \cdot V \cdot \Delta p)_e}{(A_c \cdot V \cdot \Delta p)_0} = \frac{(A_c \cdot V \cdot f \cdot L \cdot \rho \cdot V^2/D)_e}{(A_c \cdot V \cdot f \cdot L \cdot \rho \cdot V^2/D)_0} \tag{11}$$

According to the adopted assumptions, we can obtain

$$\frac{(A_c \cdot L \cdot \rho \ /D)_e}{(A_c \cdot L \cdot \rho \ /D)_0} = 1 \tag{12}$$

Substituting Eq. (12) into Eq. (11), the ratio of power consumption becomes

$$\frac{P_e}{P_0} = \frac{(f \cdot V^3)_e}{(f \cdot V^3)_0} = \frac{f_e \cdot Re^3}{f_0 \cdot Re_0^3} = \frac{f_e(Re)}{f_0(Re_0)}\left(\frac{Re}{Re_0}\right)^3 \tag{13}$$

Based on the definition of heat transfer rate, the ratio of heat transfer rate of the enhanced and reference surfaces can be presented as follows:

$$\frac{Q_e}{Q_0} = \frac{(h \cdot A \cdot \Delta t_m)_e}{(h \cdot A \cdot \Delta t_m)_0} = \frac{(Nu \cdot \lambda/D \cdot A \cdot \Delta t_m)_e}{(Nu \cdot \lambda/D \cdot A \cdot \Delta t_m)_0} \tag{14}$$

According to the assumption mentioned above, we have

$$\frac{(\lambda/D \cdot A \cdot \Delta t_m)_e}{(\lambda/D \cdot A \cdot \Delta t_m)_0} = 1 \tag{15}$$

Substituting Eq. (15) into Eq. (14), the ratio of heat transfer rate becomes

$$\frac{Q_e}{Q_0} = \frac{Nu_e}{Nu_0} \tag{16}$$

It is interesting to note that when the heat transfer rates of two surfaces are compared for surface evaluation, it is reasonable to assume the same temperature difference is being applied in the two cases. Eq. (16) is obtained under such consideration apart from the aforementioned four assumptions.

From Eq. (13) it can be seen that for the same power consumption, the ratios of friction factor of enhanced and reference surfaces at different Reynolds number becomes

$$\frac{f_e}{f_0} = \frac{f_e(Re)}{f_0(Re_0)} = \left(\frac{Re}{Re_0}\right)^{-3} \tag{17}$$

Substituting Eq. (17) into Eq. (8), we can obtain the ratio of Reynolds number under identical pumping power as follows:

$$\frac{Re}{Re_0} = \left(\frac{f_e}{f_0}\right)_{Re}^{\frac{-1}{3+m_1}} \tag{18}$$

Further, by substituting Eq. (18) into Eq. (10), we can obtain the ratio of Nusselt number under identical pump power as follows:

$$\frac{Nu_e}{Nu_0} = \frac{Nu_e(Re)}{Nu_0(Re_0)} = \left(\frac{Nu_e}{Nu_0}\right)_{Re}\left(\frac{Re}{Re_0}\right)^{m_2} = \left(\frac{Nu_e}{Nu_0}\right)_{Re}\left(\frac{f_e}{f_0}\right)_{Re}^{\frac{-m_2}{3+m_1}} \tag{19}$$

From Eqs. (16) and (19) we have

$$\frac{Q_e}{Q_0} = \frac{Nu_e}{Nu_0} = \left(\frac{Nu_e}{Nu_0}\right)_{Re}\bigg/\left(\frac{f_e}{f_0}\right)_{Re}^{\frac{m_2}{3+m_1}} \tag{20}$$

Eq. (20) is the expression of heat transfer ratio under the constraint of identical pumping power for driving the heat transfer medium. Whether the heat transfer of the enhanced surface is really enhanced under this constraint depends on the value of the ratio.

Similar formulation for the heat transfer ratio can be derived for the constraint of identical pressure drop. Based on the expression of pressure drop calculation, the ratio of pressure drop of the enhanced and the reference surfaces can be presented as

$$\frac{\Delta p_e}{\Delta p_0} = \frac{(f \cdot L \cdot \rho \cdot V^2/D)_e}{(f \cdot L \cdot \rho \cdot V^2/D)_0} \tag{21}$$

According to the assumption mentioned above, we can obtain

$$\frac{(A_c \cdot L \cdot \rho \cdot /D)_e}{(A_c \cdot L \cdot \rho \cdot /D)_0} = 1 \tag{22}$$

Substituting Eq. (22) into Eq. (21), the ratio of pressure drop of the enhanced and the reference surfaces becomes

$$\frac{\Delta p_e}{\Delta p_0} = \frac{(f \cdot V^2)_e}{(f \cdot V^2)_0} = \frac{f_e(Re)}{f_0(Re_0)}\left(\frac{Re}{Re_0}\right)^2 \tag{23}$$

From Eq. (23) it can be seen that for the same pressure drop, the ratios of friction factor of enhanced and reference surfaces at different Reynolds number becomes

$$\frac{f_e}{f_0} = \frac{f_e(Re)}{f_0(Re_0)} = \left(\frac{Re}{Re_0}\right)^{-2} \tag{24}$$

Substituting Eq. (24) into Eq. (8), the ratio of Reynolds number under identical pressure drop becomes

$$\frac{Re}{Re_0} = \left(\frac{f_e}{f_0}\right)_{Re}^{\frac{-1}{2+m_1}} \tag{25}$$

Further, by substituting Eq. (25) into Eq. (10), the ratio of Nusselt number under identical pressure drop becomes

$$\frac{Nu_e}{Nu_0} = \frac{Nu_e(Re)}{Nu_0(Re_0)} = \left(\frac{Nu_e}{Nu_0}\right)_{Re}\left(\frac{Re}{Re_0}\right)^{m_2} = \left(\frac{Nu_e}{Nu_0}\right)_{Re}\left(\frac{f_e}{f_0}\right)_{Re}^{\frac{-m_2}{2+m_1}} \tag{26}$$

Substituting Eq. (26) into Eq. (16), we can obtain

$$\frac{Q_e}{Q_0} = \frac{Nu_e}{Nu_0} = \left(\frac{Nu_e}{Nu_0}\right)_{Re}\Bigg/\left(\frac{f_e}{f_0}\right)_{Re}^{\frac{m_2}{2+m_1}} \tag{27}$$

Eq. (27) is the expression of heat transfer ratio under the constraint of identical pressure drop for driving the heat transfer medium. Whether the heat transfer of the enhanced structure is really enhanced under this constraint depends on the value of this ratio.

The heat transfer enhancement ratio between enhanced and reference surfaces for the constraint of identical flow rate case can be simply copied from Eq. (16) as follows:

$$\frac{Q_e}{Q_0} = \left(\frac{Nu_e}{Nu_0}\right)_{Re} \tag{28}$$

When experiments are conducted for the heat transfer and friction factor characteristics of enhanced and reference surfaces, the ratios of friction factor and Nusselt number at the same Reynolds numbers are often obtained. It is often required that based on such data, heat transfer performance comparisons can be examined under different constraints. Thus it will be convenient for the performance evaluation plot that the two ratios, i.e. $(f_e/f_0)_{Re}$ and $(Nu_e/Nu_0)_{Re}$ (or $(j_e/j_0)_{Re}$), are taken as the two coordinates and the comprehensive performance of the enhanced surface can be judged from the plot. For this purpose some transformation are conducted based on the three equations, i.e., Eqs. (20), (27) and (28).

The above three equations can be unified in the following form:

$$C_{Q,i} = \left(\frac{Nu_e}{Nu_0}\right)_{Re}\Bigg/\left(\frac{f_e}{f_0}\right)_{Re}^{k_i} \quad (i = P, \Delta p, V) \tag{29}$$

where P, Δp, V stand for identical pumping power, identical pressure drop and identical flow rate, respectively.

By comparison of Eq. (29) with Eqs. (20), (27) and (28), then

For identical pumping power: $C_{Q,P} = \left(\frac{Q_e}{Q_0}\right)\Big/\left(\frac{P_e}{P_0}\right) = \frac{Q_e}{Q_0}$; $k_P = \frac{m_2}{3+m_1}$ (30a)

For identical pressure drop: $C_{Q,\Delta p} = \left(\frac{Q_e}{Q_0}\right)\Big/\left(\frac{\Delta p_e}{\Delta p_0}\right) = \frac{Q_e}{Q_0}$; $k_{\Delta p} = \frac{m_2}{2+m_1}$ (30b)

For identical flow rate: $C_{Q,V} = \left(\frac{Q_e}{Q_0}\right)\Big/\left(\frac{f_e}{f_0}\right)$; $k_V = 1.0$ (30c)

By taking the logarithm of Eq. (29), we have

$$\ln\left(\frac{Nu_e}{Nu_0}\right)_{Re} = b_i + k_i \ln\left(\frac{f_e}{f_0}\right)_{Re} \tag{31}$$

where for the three constraints the constant term b_i takes the values of $\ln C_{Q,P}$, $\ln C_{Q,\Delta p}$, and $\ln C_{Q,V}$, respectively.

Eq. (31) provides the framework of our performance evaluation plot. It can be easily observed that if we take $\ln(f_e/f_0)_{Re}$, $\ln(Nu_e/Nu_0)_{Re}$ as the abscissa and ordinate, respectively, then Eq. (31) represents a straight line in such a coordinates system, for which k_i is the slope and b_i is the intercept of straight line in log–log coordinate system. Such straight lines are called performance lines. We can give both b_i and k_i some physical interpretations. The value of b_i is an indication related to the heat transfer enhancement under different constraint conditions. It represents either the ratio of heat transfer rate under the identical pumping power constraint and identical pressure drop constraint, or it represents the ratio of increase in the heat transfer rate and increase in the friction factor at the same flow rate. When $b = 0$, the straight line crosses the point of coordinate $(1,1)$ and this means that the enhanced and reference surfaces possess the same heat transfer rates under the corresponding constraint conditions. When $b > 0$, the enhanced heat transfer surface can transfer a larger heat transfer rate than that of the reference one, and when $b < 0$, the enhanced heat transfer surface transmits a lower heat transfer rate.

As far as the slope k is concerned, the magnitudes of the three constraints can be estimated as follows. For the convective heat transfer and fluid flow problems known to the authors, the range of variables m_1 and m_2 are $-1 \leqslant m_1 < 0$ and $0 < m_2 < 1$, respectively. So the following magnitude relationship can be obtained

$$0 < \frac{m_2}{3+m_1} < \frac{m_2}{2+m_1} < 1 \tag{32}$$

Thus the slope of the performance line of identical pumping power is less than that of identical pressure drop, which in turn less than that of identical flow rate. We then can conclude that: it is the easiest way to obtain the enhanced heat transfer under the identical pumping power constraint; it is relatively easy to obtain the increase of heat transfer rate under the identical pressure drop constraint; while it is quite difficult to obtain a higher heat transfer rate increase than that of friction coefficient under the same flow rate. This conclusion is consistent with our common understanding.

According to above discussion and derivations a performance evaluation plot for heat transfer enhancement techniques oriented for energy-saving is proposed in Fig. 1. In the figure the two coordinates are log–log based. The abscissa of the figure presents
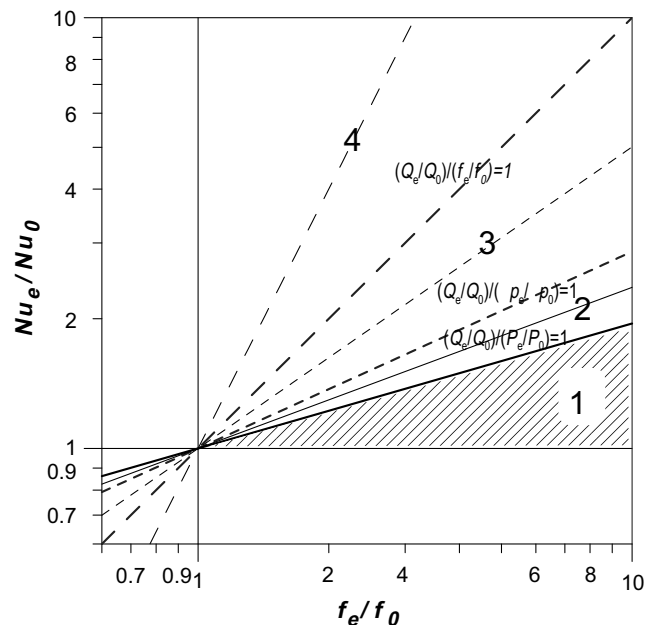

Fig. 1. A performance evaluation plot for enhancement technique oriented for energy-saving.

the friction coefficient ratio between the enhanced and reference surfaces under the same Reynolds numbers, and the ordinate presents the Nusselt number (or *j*-factor, or Stanton number) ratio between the enhanced and reference surfaces under the same Reynolds numbers. The components of this performance evaluation plot are as follows. There are two major components in the plot. One of the two major components of the plot is an array of a straight lines with different slopes through the point with coordinates (1,1). The plot can be divided into four regions indicated by the four Arabic numbers in boldface in Fig. 1. Region 1 is characterized by enhanced heat transfer without energy-saving, where

the enhancement of heat transfer rate is less than the increase of power consumption. Region 2 is featured by enhanced heat transfer with the same pump power consumption, i.e., where the enhanced surface presents higher heat transfer rate than reference one under the same pumping power consumption. In Region 3 enhanced heat transfer can be obtained with the same pressure drop, i.e., where the enhanced surface presents higher heat transfer rate than the reference one under the identical pressure drop constraint. Finally Region 4 is the most favorable one where the augmentation of heat transfer rate is more than the increase of friction coefficient under the same flow rate. The boundary line of Regions 1 and 2 is the dividing line of heat transfer enhancement
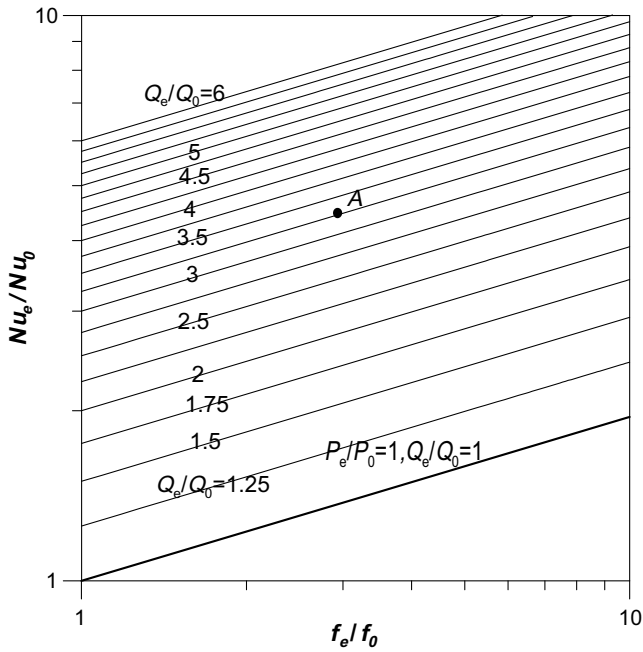

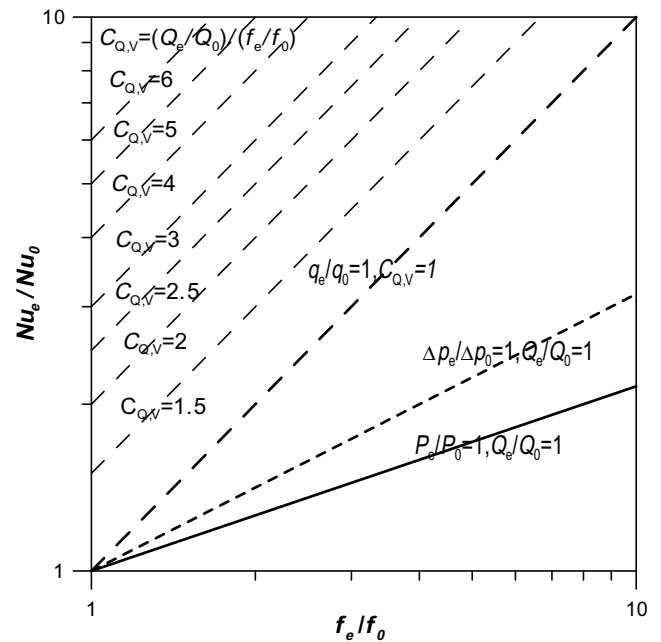**Fig. 2.** The refined contours of heat transfer enhancement ratio for identical pumping power.

Fig. 3. The contours of heat transfer enhancement ratio under identical pressure drop.

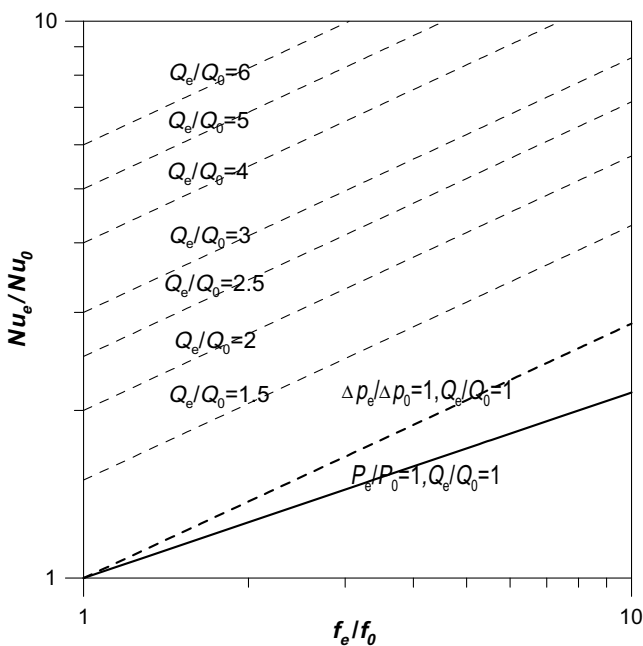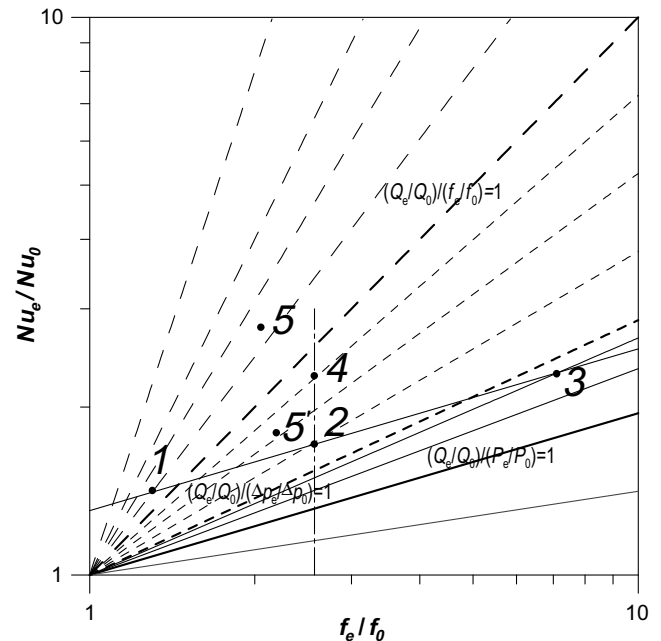**Fig. 4.** The contours of $C_{Q,V}$ under identical flow rate.

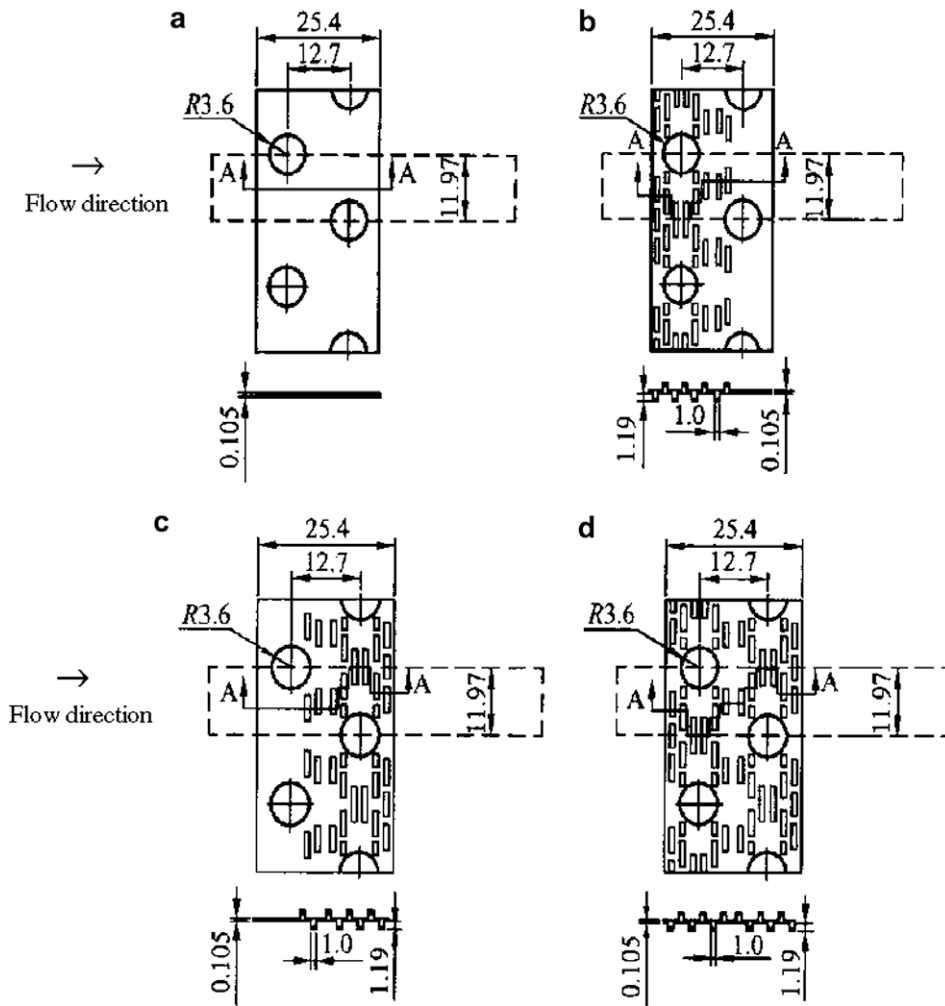**Fig. 5.** The working lines showing effectiveness of energy-saving.

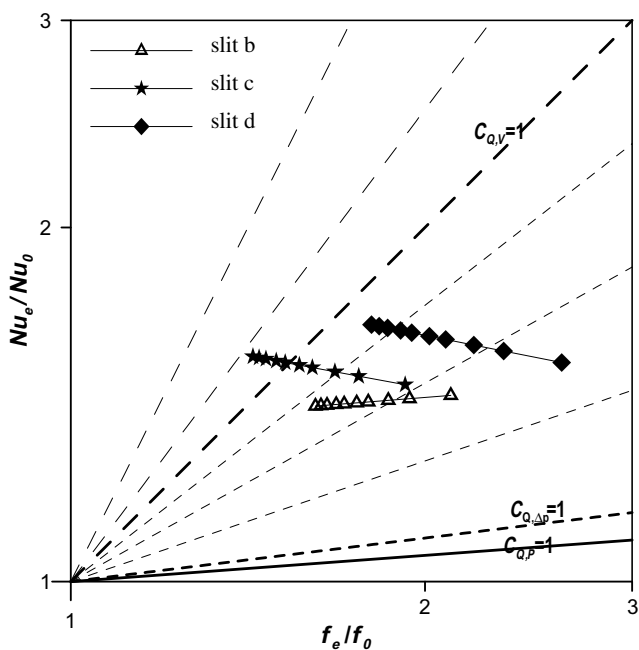**Fig. 6.** Arrangements of three kinds of slotted-fin surfaces and the referenced plate.

Fig. 7. Performance comparisons of three kinds of slotted fin in [26] for energy-saving objective.

or deterioration of the enhanced surfaces compared with the reference ones based on the identical pumping power consumption. The boundary line of Regions 2 and 3 is the dividing line of heat transfer enhancement and deterioration for the enhanced surfaces compared with the reference ones based on the identical pressure drop. The boundary line of Regions 3 and 4 is the dividing line judging the level of the ratio of increase of heat transfer rate and friction coefficient for the enhanced surfaces compared with the reference ones under the same fluid flow rate. All the above-mentioned straight lines cross the point $(1,1)$ and will be called the baselines for clarity. The boldface baselines are drawn from Eq. (31) by applying the corresponding constraint and condition. For example, the boundary line between Regions 1 and 2 is constructed under the conditions of $P_e/P_0 = 1$ and $Q_e/Q_0 = 1$. The slopes of these baselines are drawn from Eqs. (30a), (30b) and (30c), where the values of variables m_1 and m_2 come from the relevant correlations for the turbulent flow and heat transfer in smooth tubes, i.e., the value of variables m_1 and m_2 are -0.25 and 0.8, respectively [15], unless otherwise specified. The other of the two major components in this plot are the lines representing the performance of some enhancing structure, which are called the working lines. Any point on the working line is called a working point. According to the above discussion, there are three kinds of working lines corresponding to the three constraints, respectively. These three working lines are characterized by their slope (i.e., the value of k_i in Eq. (31)). As indicated above, the greater the value of the working line slope, the more se-

vere the comparison constraint. For energy-saving purposes, the larger the slope of the working line, the better the enhanced technique. As far as different points on the same working line are concerned, they have the same enhanced heat transfer ratio under corresponding friction loss constraint. Therefore, the working lines are the contours of the heat transfer enhancement ratio under different constraints.

The contours of heat transfer enhancement ratio for identical pumping power can be constructed according to Eq. (31). According to the previous analysis, the contour of heat transfer enhancement ratio is a group of parallel working lines on the log–log coordinate plot. The better the enhancement effectiveness, the larger the intercept of the straight line. The distance between the contours (i.e., working lines) can be controlled by rearranging the value of the intercept b according to actual needs. In order to show explicitly the heat transfer augmentation ratio of Point A (3.25), the contours are refined and the results are shown in Fig. 2.

The contours of heat transfer enhancement ratios for identical pressure drop and identical flow rate can be obtained in a similar way to Fig. 2 and are shown in Figs. 3 and 4.

Some applications of the present plot are illustrated in the following section.

3. Major functions of the proposed performance evaluation plot

3.1. Determining whether the enhancement technique can really save energy (pumping power)

In Fig. 1 the shaded region is the case of enhanced heat transfer without energy-saving, i.e., when a working point of an enhancement technique is located in this region the consumption of unit pumping power leads to less heat transfer rate compared with that of the reference one. Thus for energy-saving purposes the working point should be located outside the shaded region.
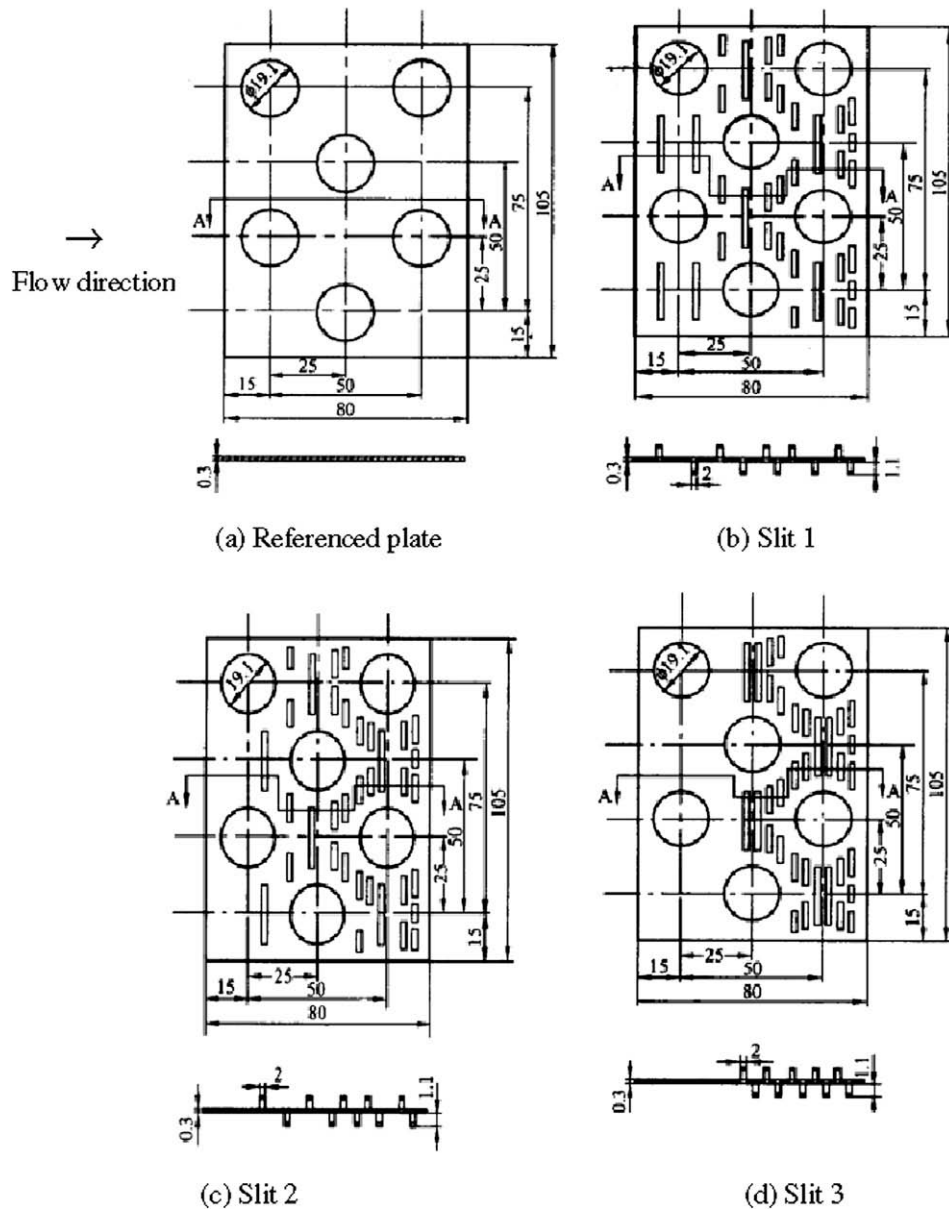

(a) Referenced plate

(b) Slit 1

(c) Slit 2

(d) Slit 3

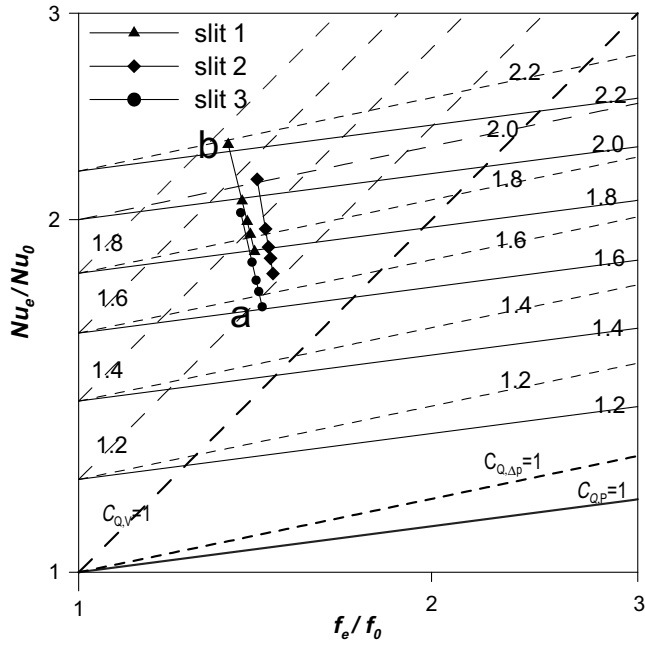**Fig. 8.** Three "front sparse and rear dense" slotted-fin surfaces and the referenced plate.

Fig. 9. The enhanced heat transfer capacity under different constraints of the slotted surfaces (data from [12]).

3.2. Showing energy-saving effectiveness

The comparison of energy-saving effectiveness of different enhanced techniques should also be conducted at certain constraints. Here, the three above-mentioned constraints are first considered. For two enhanced techniques located at the same working line it is obvious that the working point with a larger slope of its
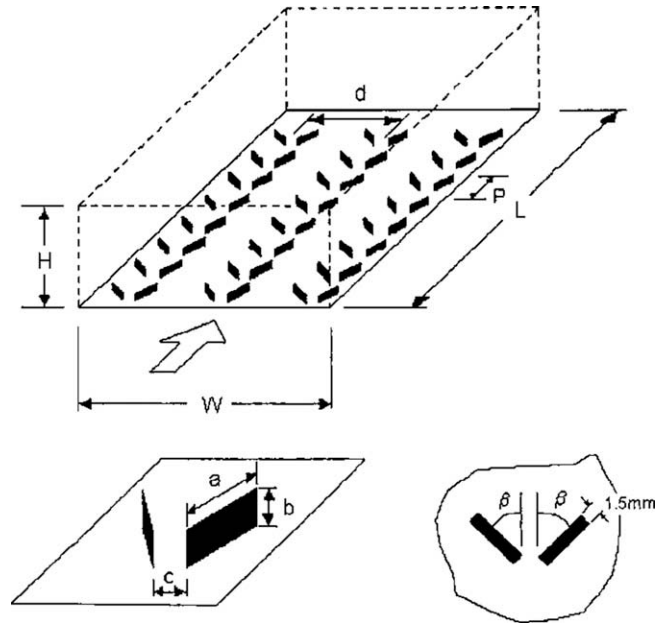

Fig. 11. Schematic diagram of the ducts with winglet disturbances.

basic line has a better energy-saving effectiveness. An example is presented in Fig. 5. In the figure three working points for the constraint of identical pumping power are shown. Points 1, 2 and 3 locate on the same working line and present the same heat transfer enhancement ratios under the identical pumping power constraint. Obviously, among the three enhanced techniques, Point 1 represents the technique with the highest energy-saving effectiveness, Point 3 has the worst energy-saving effectiveness, while Point 2 is something in between.
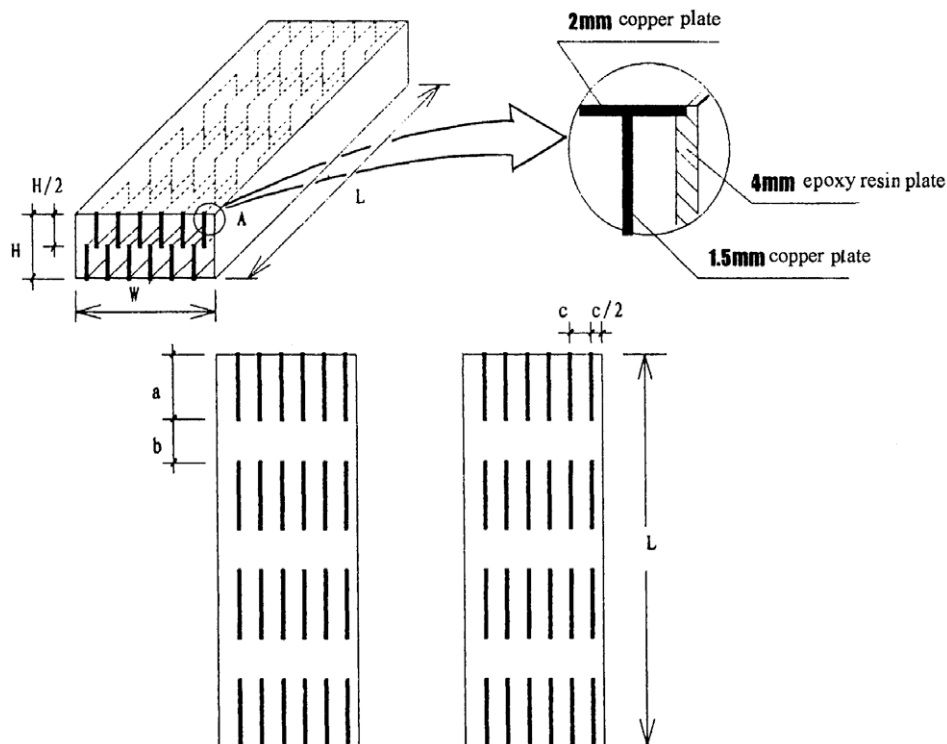

Fig. 10. Schematic diagram of the ducts with periodic rectangular fins.

Two more constraints may be added for practical usage. One is the same friction factor ratio. Point 4 and Point 2 in Fig. 5 represent such two enhanced techniques. Needless to say, Point 4 stands for the technique with a better energy-saving technique. The other condition is the same Reynolds number. In Fig. 5, Point 5 and Point 4 are supposed to be the results of two enhanced techniques at the same Re. The advantage of the technique represented by Point 5 is very clear. However, if Point 5′ and Point 4 are the results at the same Re, which technique is more effective from energy-saving point of view? From above analysis, the effectiveness of Point 4 should be regarded better because its higher heat transfer enhancement ratio.

From above illustration it can be observed that, generally speaking, the larger the basic line slope of a working point the better its energy-saving effectiveness.

It should also be indicated that if any two points in the plot are picked out without specifying a comparison condition, the energy-saving effectiveness of the two enhanced techniques can be hardly compared.

3.3. Relatively comparison between different enhanced surfaces or operational conditions

This function is actually the application of above-discussed concept. Since it is the major application of the proposed plotting technique we described it in a separate section with several examples.

3.3.1. Example 1: slotted fins with different strip locations

In actual engineering application, there are different enhanced heat transfer technologies to meet heat transfer enhancement requirements of a reference surface. We can select the better heat transfer technology through corresponding performance evaluations. The plate fin-and-tube surfaces are widely used in enhancing air-side heat transfer. For the further enhancement of heat transfer the plate fin is often slotted. For enhancing heat transfer of plate fin, three kinds of slotted fin are proposed and were tested experimentally in [26]. The slot arrangements of the three kinds of slotted fin and the reference plate fin are presented in Fig. 6. Fig. 7 presents the comparison of the three kinds of enhanced heat transfer technologies for the energy-saving objective. Three boldface baselines are drown from Eq. (31), where variables m_1 and m_2 come from the relevant correlation for laminar flow and heat transfer of air in plate-fin surface [26] with m_1 and m_2 being −0.487 and 0.186, respectively. According to the data provided in reference [26], the working points in the figure can be determined by the ratios of friction coefficient and Nusselt number between the enhanced and reference surfaces under corresponding Reynolds number. In the figure, 10 working points for slit b and slit c are presented where the corresponding Reynolds number is 350, 700, 1000, 1400, 1700, 2100, 2400, 2800, 3100 and 3400, from right to left, respectively. It should be noted since slit d has more strips than that of slit b and slit c, comparison is only conducted between slit d and slit b/c. If we connect point (1,1) with the corresponding working points of the two slits we can clearly observe that the energy-saving effectiveness of the two slotted fins are slit c, slit b in that order.

According to above discussion, it can be concluded that the slotted fin with the slots mostly in the rear part of the fin (i.e., the downstream part) is the better augment fin system.

3.3.2. Example 2: slotted fins with strips positioned according to the "Front sparse and rear dense" principle

The above example indicates that for the slotted-fin surface the slots are better to be positioned mainly in the downstream or rear part of the fin. For a specific application case, numerical investigations can be applied to determine how the slots (or strips) should

be located. In [12] three types of slotted fins are proposed characterized by the non-uniform position of strips along the flow direction. The so-called "front sparse and rear dense" positioning principle is suggested which says that the distance between two adjacent strips should be gradually reduced along the flow direction. The proposed three arrangements of strips according to this principle are shown in Fig. 8 and their heat transfer/pressure drop characteristics are tested numerically. Fig. 9 shows the working lines corresponding to the three constraints (solid line, short-dashed line and long-dashed line) drawn from Eq. (31), where variables m_1 and m_2 come from the relevant correlation for laminar flow and heat transfer of air in the plain plate fin-and-tube surfaces with m_1 and m_2 being −0.32 and 0.35, respectively [12]. According to the data provided in reference [12], five working points for the three slit fins are presented in the figure where the corresponding Reynolds number is 2100, 5600, 8000, 10,000 and 13,500, respectively. Similar discussion on the three arrangements of strips can be conducted as for the slits shown in Fig. 6. Thus slit 1 may be recommended to be used in practical application.

3.3.3. Example 3: duct with rectangular fins and winglets

One of the novel heat transfer enhancement techniques is the use of the winglet as surface turbulence or vortex promoter. Vortices are generated by flow separation. According to their axis of rotation with respect to the main flow direction, they are called longitudinal vortices while their axis of rotation is aligned with the main flow direction and transverse vortices while their axis of rotation is normal to the main flow direction. Because longitudinal vortices consist of strong swirling around an axis essentially aligned with the main flow direction, leading to a heavy fluid mixing between the core and the region near the wall. Generally, less
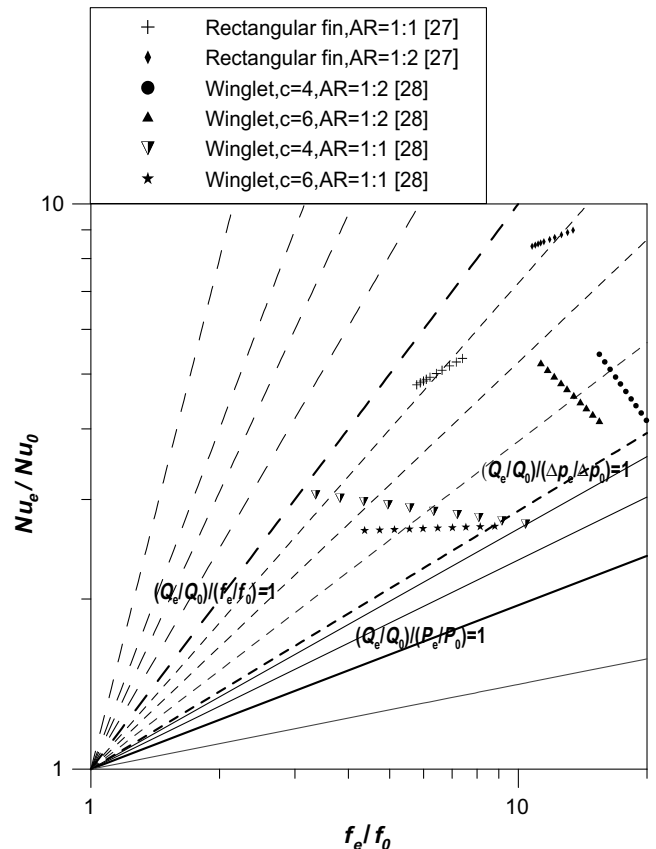

Fig. 12. Performance evaluations of ducts with rectangular fins and winglet disturbances.

energy is needed to turn the flow around an axis aligned with the main flow direction than to generate the swirl around an axis perpendicular to the main flow direction. Therefore, longitudinal vortices are more efficient for heat transfer enhancement than transverse vortices when both heat transfer and pressure drop are taken into account. Based on this, a new type of augmentation structure has been proposed and investigated in reference [27]. The passages of the structures proposed consist of a rectangular duct and internal plate fins or winglets. Figs. 10 and 11 show schematic diagrams of such structures. Yuan et al. [28] studied flow and heat transfer characteristics of ducts with internal fins and winglet disturbances.

Fig. 12 presents the performance evaluation of rectangular fins and winglet disturbances in cooling ducts for saving energy objective, where variable AR is the aspect ratio of the duct. The data in the figure come from Yuan et al. [27,28]. In the figure the working points of these enhanced surfaces mainly located in Region 3, indicating that the enhancement ratios of heat transfer rate are larger than the increases of pressure drop penalties. At the same time, we can also find from the figure that the cooling duct with rectangular fins present higher performance values than that with winglet disturbances.

3.3.4. Example 4: dimpled surface

In the past decade, a new type of enhanced surface, called dimpled surfaces, were extensively studied in the literatures [29–34]. Dimples are arrays of indentations along surfaces. Generally, these are spherical in shape, while a variety of other shapes have also been employed, ranging from triangular to tear drop. Schematic

diagrams of dimpled surfaces are shown in Fig. 13 for a flat surface and a tube [33,34]. As shown in the figure dimples do not protrude into the flow to produce significant amounts of form drag, so dimpled surfaces generally produce lower friction penalties compared to the several other types of augmentation ones. Numerous experimental investigations [29–35] were performed to study flow characteristic and heat transfer mechanism of the dimpled surface with different arrangements and geometric parameters. Flow visualization studies reveal that the flow structure in the dimple is mainly of vortex type. The vortex structure augments local and downstream Nusselt numbers. Therefore, the dimpled surface is an attractive enhanced heat transfer technology for enhancing heat transfer, especially for internal cooling technology.

Fig. 14 presents the performance comparison of different dimpled surface of turbulent flow inside cooling channel based on saving energy. The data in the figure come from references [32–36]. In the figure it can be seen that working points of these dimpled surfaces mainly located in Regions 3 and 4, implying that most of the dimpled surfaces possess high effectiveness of saving energy. At the same time, we can also find from the figure that the cooling channel with spherical dimple and protrusion on opposite surfaces presented in [36] possesses lower performance than other dimpled surface. So from the energy-saving view point, the structure of enhanced surface shown in [36] is the worst.

3.3.5. Example 5: shell-side heat transfer of helical baffled heat exchangers

In all the above-referenced cases the enhanced structure gives both larger heat transfer rate and friction factor hence the two
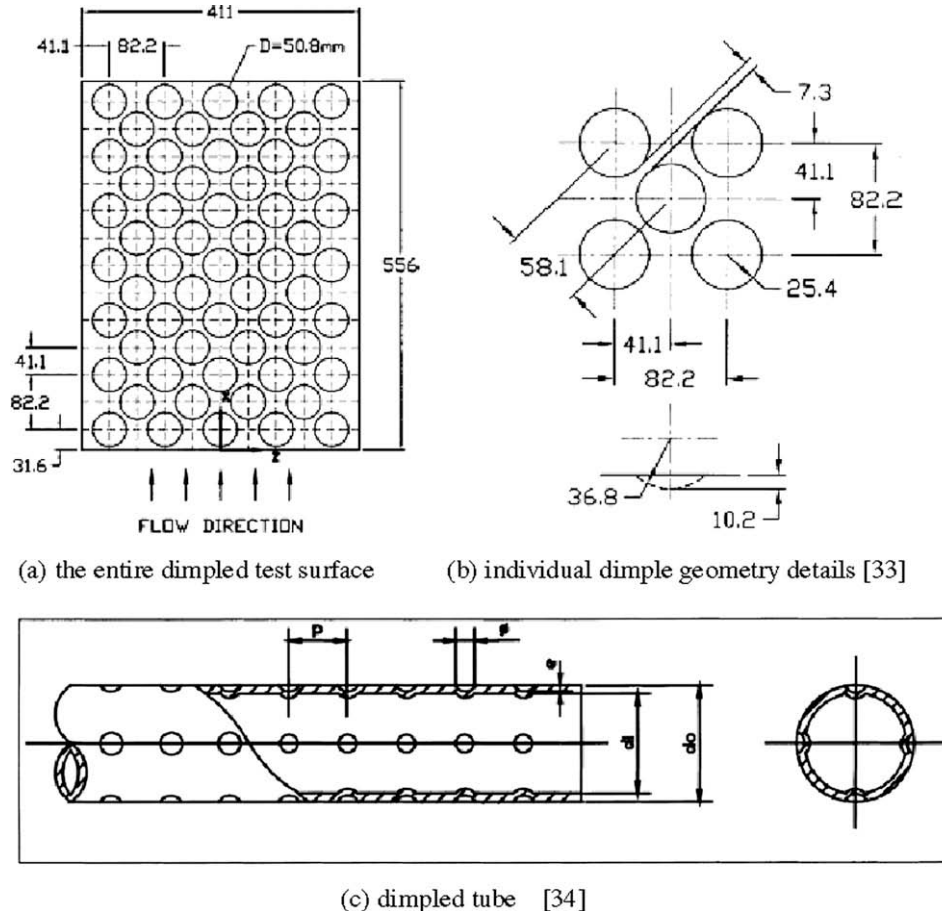

(a) the entire dimpled test surface   (b) individual dimple geometry details [33]

(c) dimpled tube [34]

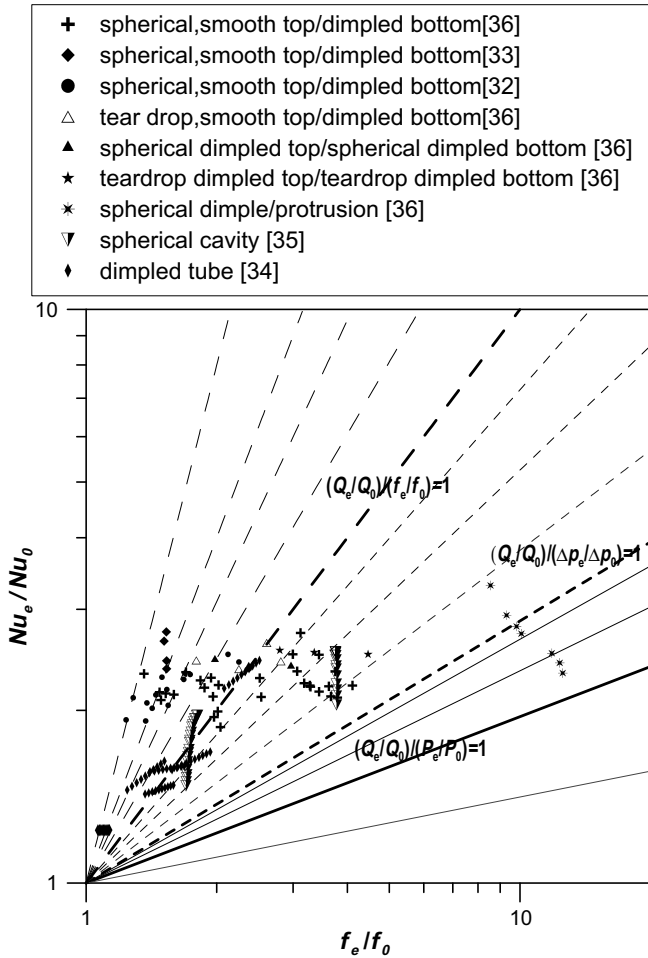Fig. 13. Schematic diagram of dimpled surface.

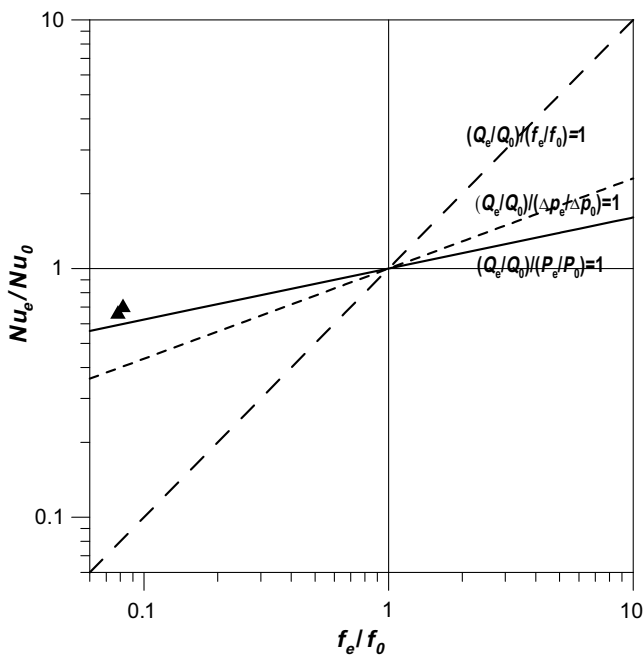**Fig. 14.** Performance evaluations of dimpled surfaces.

Fig. 15. Performance evaluations of shell-side heat transfer of helical baffle and vertical baffle heat exchangers.

ratios are greater than 1. There are some cases where the new structure leads to the reduction of both heat transfer and pressure drop, with the reduction of pressure drop being much more significant. The shell-side heat transfer occurring in the helical baffle shell-and-tube heat exchangers is one of such example. It is interesting to see whether the proposed plot technique is still applicable to such a case. For a meaningful performance comparison between the shell-and-tube heat exchangers with vertical (segmental) baffles and the helical baffles, two almost identical heat exchangers of vertical baffle type and helical baffle type were specifically made with the difference only being in the baffle type [37]. For the helical baffle its helical angle is 20°. The comparison results are presented in Fig. 15. It is interesting to note in the figure the working area is extended to the region where both the ratios of (Nu_e/Nu_0), (f_e/f_0) are less than 1. It can be easily shown that in this specially region the space under the baseline corresponding to a certain constraint is the area within which the heat transfer based on the corresponding constant has deteriorated. For example the area below the solid bold line is characterized by the deterioration of heat transfer per identical pumping power. Two typical comparison results are presented in Fig. 15. It can be seen that because the significant reduction of pressure drop, for the heat exchanger with helical baffle the shell-side heat transfer is more effective based on the identical pumping power. Thus the shell-and-tube heat exchanger with helical baffle has a more energy-saving shell-side heat transfer in this sense. It is interesting to note that in this special region, the order of implementation difficulty for the three constraints is the opposite to that, where both (Nu_e/Nu_0), (f_e/f_0) are greater than 1.0. That is the order from easy to difficult is identical flow rate, identical pressure drop and identical pumping power.

4. Conclusion

A performance evaluation plot has been proposed in this work, on the basis of the existing performance evaluation criteria analysis and four conventionally-adopted assumptions. In the plot the ratio of the friction factor of the enhanced surface over that of the reference surface and the ratio of the related heat transfer enhancement at the same Reynolds number are taken as the abscissa and ordinate, respectively. The coordinates are log–log based. From experimentally obtained data or numerically simulated results of such two ratios, a working point can be made in the plot. It is shown that the quadrant surrounded by the two coordinates can be divided by four regions corresponding to the different effectiveness of saving energy: in Region 1 heat transfer enhancement is obtained with larger pressure drop penalty such that per identical pumping power the heat transfer is deteriorated; in Region 2 heat transfer is enhanced per identical pumping power but deteriorated per identical pressured drop, in Region 3 heat transfer is enhanced per identical pressure drop, and in Region 4 the heat transfer enhancement ratio is larger than the friction factor increase ratio under identical flow rate, which is the most difficult region to reach for heat transfer enhancement study. In this plot different enhanced techniques for the same reference system can easily and clearly be compared for their energy-saving performances. Four examples are provided to show the function of such a plot. For some techniques which lead to the reduction of both heat transfer rate and friction factor, the proposed plot is still applicable. This plot will be useful in the study of heat transfer enhancement technique oriented for energy-saving purposes.

Acknowledgement

References

[1] R.L. Webb, N.H. Kim, Principles of Enhanced Heat Transfer, second ed., Taylor & Francis, Boca Raton, 2005.

[2] A.E. Bergles, Heat transfer enhancement – the maturing of second-generation heat transfer technology, Heat Transf. Eng. 18 (1) (1997) 47–55.

[3] C.C. Wang, Technology review – a survey of recent patents of fin-and-tube heat exchangers, Enhanced Heat Transf. 7 (2000) 333–345.

[4] R.K. Shah, D.P. Pekulic, Fundamentals of Heat Exchanger Design, John Wiley & Sons, Hobokin, New Jersey, 2003. pp. 696.

[5] R.L. Webb, E.R. Eckert, Application of rough surfaces to heat exchanger design, Int. J. Heat Mass Transf. 15 (1972) 1647–1658.

[6] A.E. Bergles, Techniques to enhance heat transfer, in: W.M. Rohsenow, J.P. Hartnett, Y.L. Cho (Eds.), Handbook of Heat Transfer, third ed., McGraw-Hill, New York, 1998 (Chapter 11).

[7] E.M. Sparrow, W.Q. Tao, Symmetric vs asymmetric periodic disturbances at the walls of a heated flow passage, Int. J. Heat Mass Transf. 27 (11) (1984) 2133–2144.

[8] H.Z. Huang, W.Q. Tao, An experimental study on heat/mass transfer and pressure drop characteristics for arrays of nonuniform plate length positioned obliquely to the flow direction, ASME J. Heat Transf. 115 (3) (1993) 568–575.

[9] S.S. Lue, H.Z. Huang, W.Q. Tao, Experimental study on heat transfer and pressure drop characteristics in the developing region for arrays of obliquely positioned plates of nonuniform length, Exp. Therm. Fluid Sci. 7 (1) (1993) 30–38.

[10] Z.X. Yuan, W.Q. Tao, Q.W. Wang, Numerical prediction for laminar forced convection heat transfer in parallel plate channels with streamwise-periodic rod disturbances, Int. J. Numer. Methods Fluids 28 (1998) 1371–1387.

[11] B. Yu, J.H. Nie, Q.W. Wang, W.Q. Tao, Experimental study on the pressure drop and heat transfer characteristics of tubes with internal wave-like longitudinal fins, Heat Mass Transf. 35 (1999) 65–73.

[12] Y.P. Cheng, Z.G. Qu, W.Q. Tao, Y.L. He, Numerical design of efficient slotted fin surface based on the field synergy principle, Numer. Heat Transf. Part A 45 (6) (2004) 517–538.

[13] R.K. Shah, K.A. Afimiwala, R.W. Mayne, Heat exchanger optimization, in: Proceedings of 6th International Heat Transfer Conference, vol. 4, Hemisphere, pp. 185–191.

[14] Z.G. Qu, W.Q. Tao, Y.L. He, Three dimensional numerical simulation on laminar heat transfer and fluid flow characteristics of strip fin surface with X-array arrangement of strips, ASME J. Heat Transf. 126 (2004) 697–707.

[15] Y. Sano, H. Usui, Evaluation of heat transfer promoters by the fluid dissipation energy, Scripta Publishing Co. (1982) 91–96.

[16] A. Bejan, General criterion for rating heat exchanger performance, Int. J. Heat Mass Transf. 21 (1978) 655–658.

[17] A. Bejan, Second law analysis in heat transfer, Energy 5 (1980) 721–732.

[18] R.O. William, A. Bejan, Conservation of available work (exergy) by using promoters of swirl flow in forced convection heat transfer, Energy 5 (1980) 587–596.

[19] B.H. Chen, W.H. Huang, Second-law analysis for heat transfer enhancement on a rib-type turbulence promoter, Energy 13 (2) (1988) 167–175.

[20] B.H. Chen, W.H. Huang, Performance evaluation criteria for enhanced heat transfer surface, Int. Commun. Heat Mass Transf. 15 (1988) 59–72.

[21] V.D. Zimparov, N.L. Vulchanov, Performance evaluation criteria for enhanced heat transfer surfaces, Int. J. Heat Mass Transf. 37 (12) (1994) 1807–1816.

[22] R.C. Prasad, J.H. Shen, Performance evaluation of convective heat transfer enhancement devices using exergy analysis, Int. J. Heat Mass Transf. 36 (17) (1993) 4193–4197.

[23] R.C. Prasad, J.H. Shen, Performance evaluation using exergy analysis-application to wire-coil inserts in forced convection heat transfer, Int. J. Heat Mass Transf. 37 (15) (1994) 2297–2303.

[24] R.M. Manglik, Heat transfer enhancement, in: A. Bejan, A. Kraus (Eds.), Heat Transfer Handbook, John Wiley & Son, Hobokin, New Jersey, 2003.

[25] W.J. Marner, A.E. Bergles, J.M. Chenoweth, On the presentation of performance data for enhanced tubes used in shell-and-tube heat exchanger, ASME J. Heat Transf. 105 (1983) 358–365.

[26] H. Kang, M.H. Kim, Effect of strip location on the air-side pressure drop and heat transfer in strip fin-and-tube exchanger, Int. J. Ref. 22 (1999) 302–312.

[27] Z.X. Yuan, W.Q. Wang, W.Q. Tao, Experimental study of enhanced heat transfer in ducts with periodic rectangular fins along the main flow direction, in: Heat Transfer 1998 Proceeding of 11th IHTC, Kyongju, Korea, 1998, pp. 23–28.

[28] Z.X. Yuan, W.Q. Tao, X.T. Yan, Experimental study on heat transfer in ducts with winglet disturbances, Heat Transf. Eng. 24 (2) (2003) 76–78.

[29] V.N. Afanasyev, Y.P. Chudnovsky, A.I. Leontiev, P.S. Organic, Turbulent flow friction and heat transfer characteristic for spherical cavities on a flat plate, Exp. Therm. Fluid Sci. 7 (1993) 1–8.

[30] P.M. Ligrani, G.I. Mahmood, J.L. Harrison, CM. Clayton, D.L. Nelson, Flow structure and local Nusselt number variations in a channel with dimples and protrusions on opposite walls, Int. J. Heat Mass Transf. 44 (2001) 4413–4425.

[31] P.M. Ligrani, J.L. Harrison, G.I. Mahmmod, M.L. Hill, Flow structure due to dimple depressions on a channel surface, Phys. Fluids 13 (11) (2001) 3442–3451.

[32] G.I. Mahmood, P.M. Ligrani, Heat transfer in a dimpled channel: combined influences of aspect ratio, temperature ratio, Reynolds number, and flow structure, Int. J. Heat Mass Transf. 45 (2002) 2011–2020.

[33] G.I. Mahmood, M.L. Hill, D.L. Nelson, P.M. Ligrani, H.K. Moon, B. Glezer, Local heat transfer and flow structure on and above a dimpled surface in a channel, J. Turbomach. 123 (2001) 115–123.

[34] J. Chen, Hans Müller-Steinhagen, Geoffrey G. Duffy, Heat transfer enhancement in dimpled tubes, Appl. Therm. Eng. 21 (2001) 535–547.

[35] M.Ya. Belen'kiy, M.A. Gotovskiy, B.M. Lekakh, B.S. FoKin, K.S. Dolgushin, Heat transfer augmentation using surfaces formed by a system of spherical cavities, Heat Transf. Res. 25 (2) (1993) 196–203.

[36] P.M. Ligrani, M.M. Oliveira, T. Blaskovich, Comparison of heat transfer augmentation techniques, AIAA J. 41 (3) (2003) 337–362.

[37] J.F. Zhang, Y.G. Lei, W.J. Wang, B. Li, Y.L. He, W.Q. Tao, Experimental comparison study of shell-side heat transfer of oil in helical baffle and vertical baffle heat exchangers, submitted for publication.